

## QSO ABSORPTION LINES FROM QSOS<sup>1</sup>

DAVID V. BOWEN<sup>1</sup>, JOSEPH F. HENNAWI<sup>1,2,3</sup>, BRICE MÉNARD<sup>4</sup>, DORON CHELOUCHE<sup>4,5</sup>, NAOHISA INADA<sup>6</sup>, MASAMUNE OGURI<sup>1</sup>,  
GORDON T. RICHARDS<sup>7</sup>, MICHAEL A. STRAUSS<sup>1</sup>, DANIEL E. VANDEN BERK<sup>8</sup>, DONALD G. YORK<sup>9</sup>

(Received March 24, 2006; Accepted May 30, 2006)  
*Draft version October 29, 2018*

### ABSTRACT

We present the results of a search for metal absorption lines in the spectra of background QSOs whose sightlines pass close to foreground QSOs. We detect Mg II  $\lambda\lambda 2796, 2803$  absorption in *Sloan Digital Sky Survey* (SDSS) spectra of four  $z > 1.5$  QSOs whose lines of sight pass within  $26\text{--}98 h_{70}^{-1}$  kpc of lower redshift ( $z \simeq 0.5\text{--}1.5$ ) QSOs. The 100% [4/4 pairs] detection of Mg II in the background QSOs is clearly at odds with the incidence of associated  $z_{\text{abs}} \simeq z_{\text{em}}$  systems — absorbers which exist towards only a few percent of QSOs. Although the quality of our foreground QSO spectra is not as high as the SDSS data, absorption seen towards one of the background QSOs clearly does not show up at the same strength in the spectrum of the corresponding foreground QSO. This implies that the absorbing gas is distributed inhomogeneously around the QSO, presumably as a direct consequence of the anisotropic emission from the central AGN. We discuss possible origins for the Mg II lines, including: absorption by gas from the foreground QSO host galaxy; companion galaxies fuelling the QSO through gravitational interactions; and tidal debris left by galaxy mergers or interactions which initiated the QSO activity. No single explanation is entirely satisfactory, and we may well be seeing a mixture of phenomena.

*Subject headings:* quasars:absorption lines — quasars:general

### 1. INTRODUCTION

One of the few ways to study the distribution of gas around QSOs is through absorption line studies. Until now, this has meant using the QSO itself as a background source against which absorbing gas clouds might be detected. But the origin of the narrow-line “associated”  $z_{\text{abs}} \simeq z_{\text{em}}$  systems is confusing, since even lines which have velocities  $\approx 50,000$  km s<sup>-1</sup> blueward of the emission redshift may be intrinsic to the QSO (Richards et al. 1999), at least for high ionization species. This might not be surprising, considering that the sightline looks into the heart of the AGN, but the ambiguity in translating absorption velocities into distances means we can rarely be sure where any particular line comes from. It might arise in material close to the AGN, gas ejected (and now distant) from the AGN, the host galaxy, or a companion galaxy fuelling the black hole.

If, instead, we were able to find close pairs of QSOs on the sky with very different redshifts, the background QSO could be used to probe the environment of the foreground QSO. Until recently, this experiment has been hard to do, since few such QSO pairs were known. However, the wide-area sky coverage and spectroscopic follow-up capabilities of the *Sloan Digital Sky Survey* (SDSS; York et al 2000) has resulted

in the identification of copious numbers of QSOs, making it possible to find chance alignments of quasars with very different redshifts.

In this paper we describe the results of a study designed to search for Mg II  $\lambda\lambda 2796, 2803$  Å absorption lines from foreground QSOs. Mg II is convenient because at  $z \gtrsim 0.4$  the UV doublet is redshifted into the optical region covered by SDSS spectra, a redshift low enough to investigate the environment of the foreground QSOs. Although the sample of pairs described herein is small, future studies will enable us to map the gaseous structures around QSOs, as well as improve our understanding of how quasars enrich the intergalactic medium (IGM) they inhabit.

### 2. QSO PAIRS SELECTED AND DATA ANALYSIS

The QSO pairs listed in Table 1 were discovered as part of a search for binary QSOs by Hennawi et al. (2006, hereafter H06). QSO pairs which are *not* physically associated are listed in Table 9 of H06, and for our program we selected pairs according to several criteria. First, the background QSO must have been observed by SDSS; spectroscopic confirmation of many of H06’s QSOs were made using the Apache Point Observatory (APO) 3.5 m Astrophysical Research Consortium (ARC) telescope, at a resolution and signal-to-noise (S/N) too low to allow detection of Mg II lines. Hence, APO spectra of *background* QSOs could not be used. Second, the impact parameter between the QSOs was chosen to be  $< 150 h_{70}^{-1}$  kpc<sup>11</sup>, a distance small enough to probe the inner regions of the foreground QSO’s environment. Third, the foreground QSO had to be between  $0.4 < z < 1.6$ .

The designations/positions and *g*-band magnitudes of the QSOs in Table 1 are taken from *Data Release 4* of the SDSS Archive. The APO spectra of the foreground QSOs were obtained between September 2003 and March 2004, using the Double Imaging Spectrograph (DIS) configured with a 1.5

<sup>1</sup> Based in part on observations obtained with the Apache Point Observatory 3.5-meter telescope, which is owned and operated by the Astrophysical Research Consortium.

<sup>1</sup> Princeton University Observatory, Princeton, NJ 08544

<sup>2</sup> Hubble Fellow

<sup>3</sup> Dept. of Astronomy, University of California, Berkeley, CA 94720

<sup>4</sup> Institute for Advanced Study, Einstein Drive, Princeton, NJ 08540

<sup>5</sup> Chandra Fellow

<sup>6</sup> Institute of Astronomy, Faculty of Science, University of Tokyo, 2-21-1 Osawa, Mitaka, Tokyo 181-0015, Japan

<sup>7</sup> Dept. of Physics and Astronomy, Johns Hopkins University, 3400 N. Charles St., Baltimore MD 21218

<sup>8</sup> Department of Astronomy and Astrophysics, The Pennsylvania State University, 525 Davey Laboratory, University Park, PA 16802

<sup>9</sup> Dept. of Astronomy and Astrophysics, University of Chicago, Enrico Fermi Institute, 5640 South Ellis Avenue, Chicago, IL 60637.

<sup>11</sup>  $h_{70} = H_0/70$  km s<sup>-1</sup> Mpc<sup>-1</sup>,  $\Omega_m = 0.3$  and  $\Omega_\lambda = 0.7$ .

TABLE 1  
 QSO-QSO PAIRS

Background QSO/ Foreground QSO	Plate–MJD–fibre	$z_{\text{em}}$	$g$ -band psf mag	$M_B$	$\rho$ (")	$\rho$ ( $h_{70}^{-1}$ kpc)	$z_{\text{abs}}$	$W_r$ (Mg II) <sup>a</sup>		$W_r(\text{assoc})^b$ (Å)
								$\lambda 2796$ (Å)	$\lambda 2803$ (Å)	
SDSS J095454.99+373419.9	1596–52998–330	1.884	18.9	...	3.1	26	1.5496	$1.10 \pm 0.17$	$0.33 \pm 0.19$	...
SDSS J095454.73+373419.7	...	1.544	19.6	–24.8	...	...	...	...	...	< 0.42
SDSS J083649.55+484154.0	0550–51959–426	1.711	18.5	...	4.1	29	0.6563	$1.90 \pm 0.11$	$1.24 \pm 0.12$	...
SDSS J083649.45+484150.0	...	0.657	19.3	–23.1	...	...	...	...	...	< 0.56
SDSS J231253.03+144453.4	0743–52262–596	1.521	17.8	...	6.4	47	0.7672	$0.39 \pm 0.12$	$0.19 \pm 0.12$	...
SDSS J231252.79+144458.6	...	0.768	20.3	–22.7	...	...	...	...	...	< 1.16
SDSS J211230.33–063332.1	0638–52081–551	1.544	19.5	...	15.2	98	0.5411	$1.59 \pm 0.35$	$1.69 \pm 0.35$	...
SDSS J211229.31–063331.4	...	0.551	20.2	–22.1	...	...	...	...	...	< 1.60

<sup>a</sup>Rest equivalent widths of Mg II absorption in the background (SDSS) QSO spectrum.

<sup>b</sup> $2\sigma$  upper limit to the rest equivalent width of associated ( $z_{\text{abs}} \simeq z_{\text{em}}$ ) absorption in the foreground (APO) QSO spectrum.

arcsec slit and low dispersion gratings, giving a resolution of 7–8 Å FWHM (see H06 for further details). The redshifts of the foreground QSOs are taken from Table 9 of H06, while their absolute  $B$ -band magnitudes come from the cross-filter  $K$ -correction  $K_B(z)$  between SDSS  $i$ -band and Johnson  $B$ -band computed from the composite quasar spectrum of Vanden Berk et al. (2001) and Johnson- $B$  and SDSS- $i$  filter curves. Background QSO spectra were retrieved from the SDSS Archive. At the wavelengths where Mg II is expected the resolution of the SDSS spectra is 2.2 Å at 4500 Å, and 3.6 Å at 7000 Å, FWHM, or  $\sim 150$  km s<sup>–1</sup>.

Mg II lines were detected in the spectra of all four background QSOs. The SDSS spectra are plotted in Fig. 1, along with the lower resolution APO spectra of the foreground quasars. The redshift of the Mg II absorption is remarkably close to the systemic redshift of the QSO for three of the pairs. Fig. 1 shows that the Mg II emission line profile of SDSS J231252.79+144458.6 appears offset from the absorption, but the redshift of the QSO is actually derived from a narrow [O II]  $\lambda 3727$  line, which should give a more reliable systemic redshift. The difference in velocity between absorption and emission for SDSS J211229.31–063331.4 is 1900 km s<sup>–1</sup>, but the blue wing of the emission line appears quite non-Gaussian, and may be affected by associated Mg II absorption (see §3).

To measure the properties of the absorption lines, we normalized the QSO continua by defining a least-square fit of Legendre polynomials to the continuum flux (Sembach & Savage 1992). This results in a best-fit to the continuum, along with upper and lower continua which represent the  $\pm 1\sigma$  errors in the adopted continuum. Line wavelengths were measured by fitting Gaussian profiles to the data. The final redshifts of the absorption systems were determined by averaging the redshift of each line of the doublet. Line equivalent widths (EWs) were measured in the standard way:  $W = \sum_i^n (1 - F_i) \delta\lambda$ , where  $F_i$  is the normalized flux at the  $i$ 'th pixel,  $\delta\lambda$  is the wavelength dispersion, and the sum is calculated over  $n$  pixels. The variance from Poisson noise is given by  $\sigma^2(W) = \sum_i^n (\sigma_i \delta\lambda)^2$ . Error arrays from the SDSS pipeline provided values of  $\sigma_i$ . We took  $n$  to be a value four times the resolution, or nine pixels. Rest frame EWs ( $W_r$ ) are given in Table 1. Errors from continuum fitting were measured by taking the difference between  $W$  measured from the best-fit continuum and  $W$  measured from the spectrum normalized by the upper and lower  $1\sigma$  error continua. A final EW error was calculated from the quadratic sum of the Poisson noise

error and the continuum error.

The ratio  $\text{DR} = W_r(\lambda 2796)/W_r(\lambda 2803)$  towards SDSS J095454.99+373419.9 is  $3.3 \pm 2.2$ , which is consistent with the value of 2.0 for this doublet in optically thin gas to within the  $1\sigma$  errors; we also detect strong C IV  $\lambda\lambda 1548, 1550$  absorption at precisely the same redshift as the Mg II line (Fig. 1), which supports the reality of the detection. Towards SDSS J211230.33–063332.1, there appears to be an additional absorption component redward of the Mg II doublet. This may simply be from Poisson noise, but the feature is significant at the  $3\sigma$  level. It may therefore be more indicative of additional high velocity absorption from the complex. Nevertheless, the identification of Mg II at  $z = 0.5411$  seems secure, since the two members of the doublet are detected at a  $4.5\sigma$  significance, and the wavelengths of the two lines give identical redshifts to within 20 km s<sup>–1</sup>, or one-eighth of a resolution element, assuming the lines are the two members of the Mg II doublet.

We also calculated  $2\sigma$  rest-frame EW limits,  $W_r(\text{assoc})$ , for associated absorption, i.e., absorption in the foreground QSO spectra at their emission redshifts in the lower resolution APO spectra. Values of  $W_r(\text{assoc})$  are given in Table 1, though these may under-represent the true values; at the resolution of the APO spectra, absorption lines may not be apparent at the peak of an emission line, and the continuum placement may be under-estimated.

### 3. RESULTS

Fig. 1 shows that Mg II absorption is detected close to the redshift of each of the four foreground QSOs. No other  $z < 1.6$  pairs for which the redshift of the foreground QSO was confirmed spectroscopically were available, so there are no examples of QSOs probed within 98  $h_{70}^{-1}$  kpc which failed to show Mg II absorption in background QSO spectra. This suggests that the Mg II cross-section around QSOs is high out to 98  $h_{70}^{-1}$  kpc, although the statistics are clearly very poor considering the small number of pairs studied. The Mg II absorbing galaxies found by Steidel (1995) extend only half as far, although our results are more consistent with recent work by Churchill et al. (2005) and Zibetti et al. (2005). Given the paucity of Mg II systems along random QSO sightlines —  $< 1$  per unit redshift for lines with the strengths listed in Table 1 (e.g. Nestor et al. 2005) — the absorption is unlikely to merely be a chance alignment in redshift space.

We also find that the absorption towards the background QSO SDSS J083649.55+484154.0 — that is, in the direction

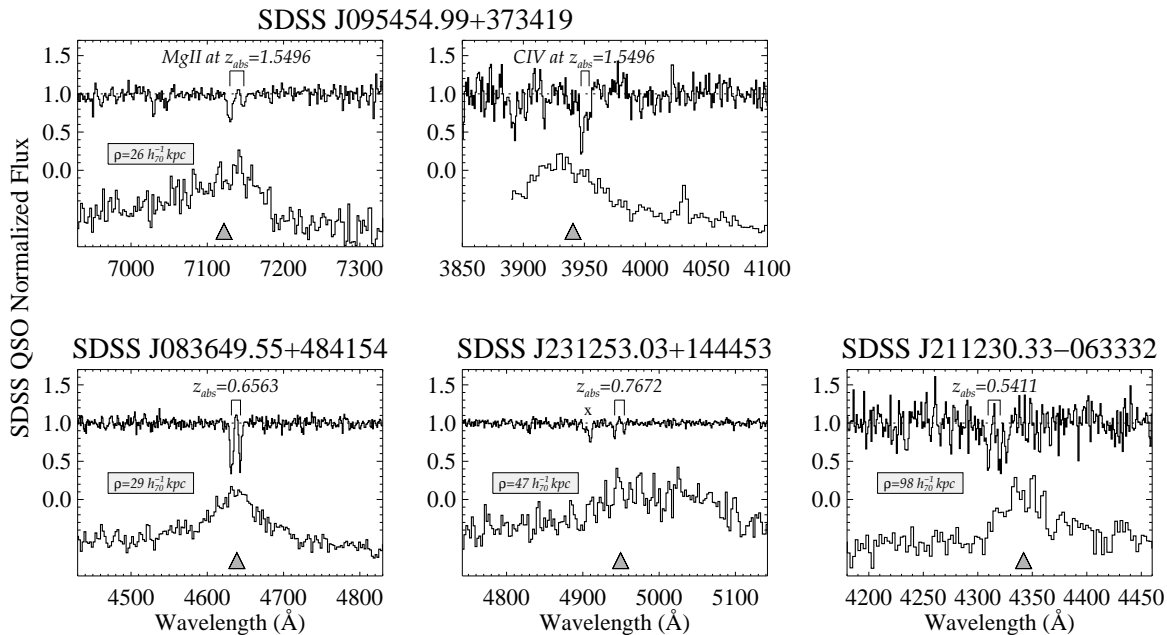


FIG. 1.— Four panels showing Mg II absorption in the normalized background (SDSS) QSO spectrum (top of each panel), and one panel showing C IV absorption towards SDSS J095454.99+373419.9. Mg II (and C IV) emission in the foreground (APO) QSO spectrum is plotted at the bottom of each panel. The foreground QSO spectra are not flux calibrated, and are scaled as needed. Tick marks show the *predicted* position of Mg II (and C IV) given the designated redshift. The ‘X’ marked in the spectrum of SDSS J231253.03+144453.4 is an Fe II  $\lambda$ 2382 line at  $z = 1.0604$ . Triangles represent the expected position of the narrow absorption lines in the background QSO, as well as the Mg II emission of the foreground QSO, based on the systemic redshift of the foreground QSO.

*transverse* to the foreground QSO — does not appear at  $z_{\text{abs}} \simeq z_{\text{em}}$  along the sightline to the foreground quasar — i.e. in the *radial* direction of the foreground QSO. The Mg II absorption is strong ( $W_r = 2 \text{ \AA}$ ), and absorption of similar strength would be detected in the APO spectrum of the foreground QSO, which has a  $2\sigma$  rest EW limit of  $W_r(\text{assoc}) \approx 0.6 \text{ \AA}$ . For the three other QSO pairs the lower resolution and S/N of the APO spectra make it hard to detect absorption in the radial direction with the same strength as that seen in the transverse direction. The asymmetric emission line profile of the foreground QSO SDSS J211229.31–063331.4 could, however, be the result of intrinsic absorption, and might explain the large velocity difference between absorption and emission.

Our observations suggest that the incidence of Mg II absorbing gas measured transversely to a QSO is quite different from that measured radially towards a QSO. The incidence of associated ( $z_{\text{abs}} \simeq z_{\text{em}}$ ) narrow-line Mg II absorption with strengths similar to those detectable in SDSS data is  $< 11 \%$  (Steidel & Sargent 1992; Aldcroft et al. 1994). In comparison, we find Mg II in 4/4 systems in the transverse direction, which appears to indicate that there exists a deficit of Mg II gas in the radial direction to QSOs relative to that seen in the transverse direction. The difference is likely related to the anisotropic radiation field of the QSO. Although the existence of Mg II in a gas cloud depends on many factors (strength of the ionizing field, gas density, etc.) the simplest, qualitative explanation for our results is that the AGN radiation field strongly ionizes gas in the radial direction so that Mg II is not present, whereas gas situated in the transverse direction does not see the same intense radiation, and is therefore less highly ionized.

#### 4. DISCUSSION

What are the possible origins for the Mg II absorbing gas seen in the transverse direction towards the background QSOs? One possibility is that Mg II arises in host-galaxy

disks; the three  $z < 1$  QSOs in Table 1 lie at the faint end of the QSO luminosity function (Richards et al. 2005), and hosts of low-luminosity, radio-quiet<sup>12</sup> QSOs often reside in disk galaxies (Hamilton et al. 2002). SDSS J083649.45+484150.0 is probed at an impact parameter of  $29 h_{70}^{-1} \text{ kpc}$ ; the background QSO spectrum shows strong Fe II  $\lambda$ 2382 ( $W_r = 1.53 \pm 0.13 \text{ \AA}$ ) and Fe II  $\lambda$ 2600 ( $1.01 \pm 0.11 \text{ \AA}$ ) lines. The resulting Mg II ( $\lambda$ 2796)/Fe II ( $\lambda$ 2600) rest EW ratio of  $1.9 \pm 0.2$  means that there is a  $\simeq 40 \%$  probability that this absorber is also a damped Lyman- $\alpha$  system, with  $\log N(\text{H I}) \gtrsim 20$  (Rao et al. 2006). Even if  $N(\text{H I})$  is somewhat less than this, the strengths of the absorption lines suggest that they might arise in a galactic disk, since disks are indicative of regions of high column densities.

Conversely, the absorption from SDSS J211229.31–063331.4 is unlikely to arise in a host disk; although the absorption is strong, few galaxy disks with radii of  $98 h_{70}^{-1} \text{ kpc}$  are known. Of course, many QSOs are not hosted by disk galaxies at all. QSOs more luminous than  $M_V < -24$  are typically found in massive elliptical galaxies brighter than  $L^*$  (e.g. Dunlop 2004, and refs. therein), and one of our foreground QSOs, SDSS J095454.73+373419.7, is indeed more luminous than this. Floyd et al. (2004) have shown that the average half-light radius  $\langle R_{1/2} \rangle$  is  $\sim 14 h_{70}^{-1} \text{ kpc}$  for the elliptical hosts of these bright QSOs. The radius at which SDSS J095454.73+373419.7 is probed,  $26 h_{70}^{-1} \text{ kpc}$ , is only twice  $\langle R_{1/2} \rangle$ , and is consistent with  $R_{1/2}$  for some of the larger ellipticals. However, it is unclear whether strong Mg II absorption could be associated with a giant elliptical galaxy. Some ellipticals contain small amounts of cold gas near their centers, but most of the gas

<sup>12</sup> None of the foreground QSOs are detected in the 1.4 GHz NRAO/VLA Sky Survey (NVSS) catalog (Condon et al. 1998); a 28 mJy source is detected in the field of SDSS J231253.03+144453.4, but it appears to be the background QSO.

is expected to be too hot for Mg II to survive. There exists little data on the absorbing properties of ellipticals. At low redshift, no Mg II absorption was seen in UV spectra of SN 1998S which exploded in the Fornax elliptical NGC 1380 (Bowen et al. 1995), although the lack of absorption may have been due to a short path length through the galaxy to the supernova. On the other hand, Steidel et al. (1994) found that *all* types of galaxies were likely to be Mg II absorbers.

A second possible explanation for the Mg II absorption is that the lines arise from a companion galaxy of the foreground QSO. Low redshift QSOs reside in galaxy groups of moderate richness (Bahcall & Chokshi 1991) with the highest overdensities occurring within  $\sim 100$  kpc (Fisher et al. 1996; Serber et al. 2006); hence the probability of intercepting a galaxy in the same group as a QSO is likely to be high. Mg II might arise from a companion galaxy directly interacting with the quasar. QSO activity probably begins when galaxies merge, and quasar hosts are often found with close companions (Yee 1987; Bahcall et al. 1997), even if tidal remnants are not always apparent (Lim & Ho 1999). Interactions are certainly an excellent method of distributing gas over a large area. Absorption lines have been recorded from tidal debris (Bowen et al. 1994; de Boer et al. 1993; Norman et al. 1996), and enrichment of the IGM by tidal stripping has been invoked to explain absorption systems that have near solar metallicities, but for which no absorbing galaxy can be found close to the sightline (Jenkins et al. 2005; Aracil et al. 2006).

Finally, we note that numerical simulations predict that supermassive black holes form when galaxies of similar mass merge (Kauffmann & Haehnelt 2000; Volonteri et al. 2003; Menci et al. 2003); again, the merger of two galaxies may produce tidal debris over a wide area. In addition, inflows of gas onto a black hole may produce intense star formation and the onset of powerful winds (Di Matteo et al. 2005; Hopkins et al. 2005, and refs. therein). Intercepting such a wind might give rise to absorption lines; it could also explain the large velocity difference between emission and absorption in SDSS J211230.33–063332.1 (if the systemic redshift of the foreground QSO is correct). Whether such an explanation is tenable obviously depends on the morphology of the wind and its orientation to the background QSO sightline.

#### 5. FUTURE WORK

Much work remains in order to characterize the Mg II cross-section of QSOs. Obviously, a sample of four QSO pairs is

too small to enable us to draw firm conclusions, and observations of more pairs are needed to test if the  $\sim 100\%$  covering factor is a robust estimate, and whether this changes depending on the strength of the Mg II lines selected. Similarly, we need to probe beyond  $98 h_{70}^{-1}$  kpc to find the limit of the Mg II absorption. With the numerous QSOs detected by the SDSS, searching for Mg II at larger radii is now possible, and will be the subject of a future paper. Deep, high resolution imaging should help reveal the origin of the absorption if, e.g., companion galaxies to the foreground QSOs, or evidence for previous mergers or interactions, can be found. Selecting foreground QSOs with  $z \ll 1$  makes detecting faint companions or asymmetric morphologies more feasible. Echelle-resolution spectra of background QSOs will be important for finding complex velocity structure in the absorbing gas, which may be related to its origin in a wind or in tidal debris.

Spectra of foreground QSOs at resolutions and S/N comparable to SDSS spectra will also be important for finding differences between absorption in the radial and transverse directions of QSOs. Since differences are likely to be associated with changes in the ionization conditions of the gas, observations of other higher ionization absorption lines in both background and foreground QSO spectra will be pertinent. As noted in §2, the Mg II system towards the background QSO SDSS J095454.99+373419.9 shows strong C IV absorption, although we have insufficient data to know whether C IV absorption is also seen towards the foreground QSO in the radial direction. Such studies can be carried out for high- $z$  foreground QSOs when the high ionization lines are redshifted beyond the atmospheric cut-off.

D.V.B is funded through LTSA NASA grant NNG05GE26G. J.F.H is supported through NASA Hubble Fellowship grant 01172.01-A, awarded by the Space Telescope Science Institute. B.M. acknowledges financial support from the F. Gould Foundation. D.C. is supported by NASA through Chandra Postdoctoral Fellowship award PF4-50033. M.A.S. is supported through NSF grant AST-0307409. Funding for the SDSS Archive has been provided by the Alfred P. Sloan Foundation, the Participating Institutions, NASA, the National Science Foundation, the Dept. of Energy, the Japanese Monbukagakusho, and the Max Planck Society.

#### REFERENCES

- Aldcroft, T. L., Bechtold, J., & Elvis, M. 1994, *ApJS*, 93, 1  
 Aracil, B., Tripp, T. M., Bowen, D. V., Prochaska, J. X., Chen, H.-W., & Frye, B. L. 2006, *MNRAS*, 154  
 Bahcall, J. N., Kirhakos, S., Saxe, D. H., and Schneider, D. P. 1997, *ApJ*, 479, 642  
 Bahcall, N. A. & Chokshi, A. 1991, *ApJ*, 380, L9  
 Bowen, D. V., Blades, J. C., & Pettini, M. 1995, *ApJ*, 448, 634  
 Bowen, D. V., Roth, K. C., Blades, J. C., & Meyer, D. M. 1994, *ApJ*, 420, L71  
 Churchill, C. W., Kacprzak, G. G., & Steidel, C. C. 2005, in *IAU Colloq. 199: Probing Galaxies through Quasar Absorption Lines*, 24–41  
 Condon, J. J., Cotton, W. D., Greisen, E. W., Yin, Q. F., Perley, R. A., Taylor, G. B., & Broderick, J. J. 1998, *AJ*, 115, 1693  
 de Boer, K. S., Pascual, P. R., Wamsteker, W., Sonneborn, G., Fransson, C., Bomans, D. J., & Kirshner, R. P. 1993, *A&A*, 280, L15  
 Di Matteo, T., Springel, V., & Hernquist, L. 2005, *Nature*, 433, 604  
 Dunlop, J. S. 2004, in *Carnegie Observatories Astrophysics Series, Vol. 1, Coevolution of Black Holes and Galaxies*, ed. H. L. C. (Cambridge: Cambridge Univ. Press), 341  
 Fisher, K. B., Bahcall, J. N., Kirhakos, S., & Schneider, D. P. 1996, *ApJ*, 468, 469  
 Floyd, D. J. E., Kukula, M. J., Dunlop, J. S., McLure, R. J., Miller, L., Percival, W. J., Baum, S. A., & O’Dea, C. P. 2004, *MNRAS*, 355, 196  
 Hamilton, T. S., Casertano, S., & Turnshek, D. A. 2002, *ApJ*, 576, 61  
 Hennawi, J. F. et al 2006, *AJ*, 131, 1  
 Hopkins, P. F., Hernquist, L., Cox, T. J., Di Matteo, T., Martini, P., Robertson, B., & Springel, V. 2005, *ApJ*, 630, 705  
 Jenkins, E. B., Bowen, D. V., Tripp, T. M., & Sembach, K. R. 2005, *ApJ*, 623, 767  
 Kauffmann, G. & Haehnelt, M. 2000, *MNRAS*, 311, 576  
 Lim, J. & Ho, P. T. P. 1999, *ApJ*, 510, L7  
 Menci, N., Cavaliere, A., Fontana, A., Giallongo, E., Poli, F., & Vittorini, V. 2003, *ApJ*, 587, L63  
 Nestor, D. B., Turnshek, D. A., & Rao, S. M. 2005, *ApJ*, 628, 637  
 Norman, C. A., Bowen, D. V., Heckman, T., Blades, C., & Danly, L. 1996, *ApJ*, 472, 73  
 Rao, S. M., Turnshek, D. A., & Nestor, D. B. 2006, *ApJ*, 636, 610  
 Richards, G. T. et al 2005, *MNRAS*, 360, 839

- Richards, G. T., York, D. G., Yanny, B., Kollgaard, R. I., Laurent-Muehleisen, S. A., & vanden Berk, D. E. 1999, *ApJ*, 513, 576
- Sembach, K. R. & Savage, B. D. 1992, *ApJS*, 83, 147
- Serber, W., Bahcall, N., Ménard, B., & Richards, G. 2006, astro-ph/0601522
- Steidel, C. C. 1995, in *QSO Absorption Lines, Proceedings of the ESO Workshop Held at Garching, Germany, 21 - 24 November 1994*, ed. G. Meylan. Springer-Verlag Berlin Heidelberg, New York, 139
- Steidel, C. C., Dickinson, M., & Persson, S. E. 1994, *ApJ*, 437, L75
- Steidel, C. C. & Sargent, W. L. W. 1992, *ApJS*, 80, 1
- Vanden Berk, D. E. et al 2001, *AJ*, 122, 549
- Volonteri, M., Haardt, F., & Madau, P. 2003, *ApJ*, 582, 559
- Yee, H. K. C. 1987, *AJ*, 94, 1461
- York et al. 2000, *AJ*, 120, 1579
- Zibetti, S., Ménard, B., Nestor, D., & Turnshek, D. 2005, *ApJ*, 631, L105